condensed matter

MDPI

Article

Possible Manifestation of Q-Ball Mechanism of High-T_c Superconductivity in X-ray Diffraction

Sergei Mukhin

Theoretical Physics and Quantum Technologies Department, NUST "MISIS", Leninskiy Ave. 4, 119049 Moscow, Russia; si.muhin@misis.ru; Tel.: +7-495-955-0062

Abstract: It is demonstrated, that recently proposed by the author Q-ball mechanism of the pseudogap state and high-Tc superconductivity in cuprates may be detected in micro X-ray diffraction, since it imposes inverse correlations between the size and scattering intensities of the Q-ball charge-density-wave (CDW) fluctuations in these compounds. The Q-ball charge Q gives the number of condensed elementary bosonic excitations in a CDW fluctuation of finite amplitude. The attraction between these excitations inside Euclidean Q-balls is self-consistently triggered by the simultaneous condensation of Cooper/local pairs. Euclidean Q-ball solutions, analogous to the famous Q-balls of squarks in the supersymmetric standard model, arise due to the global invariance of the effective theory under the $U(1)$ phase rotation of the Fourier amplitudes of the short-range CDW fluctuations. A conserved 'Noether charge' Q along the Matsubara time axis equals $Q \propto TM^2V$, where the temperature T, Q-ball's volume V, and fluctuation amplitude M enter. Several predictions are derived in an analytic form that follow from this picture. The conservation of the charge Q leads to an inverse proportionality between the volume V and X-ray scattering intensity $\sim M^2$ of the CDW puddles found in micro X-ray scattering experiments. The theoretical temperature dependences of the most probable Q value of superconducting Q-balls and their size and scattering amplitudes fit well the recent X-ray diffraction data in the pseudogap phase of high-Tc cuprates.

Keywords: Cooper-pairing 'glue'; Euclidean Q-balls; micro X-ray diffraction; 'nesting'; high-temperature superconductivity

PACS: 74.20.-z; 71.10.Fd; 74.25.Ha

check for updates

Citation: Mukhin, S. Possible Manifestation of Q-Ball Mechanism of High-T_c Superconductivity in X-ray Diffraction. *Condens. Matter* **2023**, *8*, 16. https://doi.org/10.3390/condmat8010016

Academic Editors: Alexander A. Golubov and Atsushi Fujimori

Received: 16 December 2022
Revised: 15 January 2023
Accepted: 25 January 2023
Published: 28 January 2023

Copyright: © 2023 by the author. Licensee MDPI, Basel, Switzerland. This article is an open access article distributed under the terms and conditions of the Creative Commons Attribution (CC BY) license (https://creativecommons.org/licenses/by/4.0/).

1. Introduction

Recently, a theory of a Q-ball mechanism of a pseudogap (PG) phase and high-T_c superconductivity in cuprates was proposed by the author [1,2] in order to account theoretically for the most salient features of these and newly found compounds. The Q-balls theory predicts the direct manifestation of Q-balls in X-ray diffraction experimental results on high-Tc cuprate superconductors in the pseudogap phase [3,4]. The same Q-ball mechanism also predicts a diamagnetic moment of the Q-ball gas as a function of a magnetic field above T_c, see arXiv:2108.10372 (2021) in [1], that favourably compares with experimental data in cuprates [5]. In addition, the theory [1] predicts the linear dependence of the superconducting transition temperature T_c on the density n_s of the local Cooper-pair Bose condensate found experimentally [6] when the Q-ball radius approaches infinity at the bulk superconducting transition. Before passing to the description of the Q-balls picture, it is useful to shortly mention some major features of the unconventional superconductors. These were found during the last 36 years since the first discovery in 1986 of high-temperature superconductivity (HTS) in the doped copper oxide perovskites $La_{2-x}Ba_xCuO_4$ [7] below $T_c \approx 30$ K, followed by the steep rise of the measured T_c up to $T_c \approx 135$ K, and under pressure up to $T_c \approx 164$ K, in another perovskite $HgBa_2Ca_2Cu_3O_{8+\delta}$ [8]. In parallel to

the discoveries in cuprates, a superconductivity below $T_c = 39$ K was found in magnesium diboride MgB_2 [9], as well as in iron-based superconductors, where the T_c values approach 60 K [10,11]. The angle-resolved photoemission experiments (ARPES) from Bi2201 [12] revealed that at temperatures below T^*, and well above the superconducting T_c, a pseudogap appears in the remnant fermionic Fermi-surface antinodal regions. The scanning tunnelling microscopy (STM) reveals both the particle–hole symmetry breaking and pronounced spectral broadening indicative of a spatial state distinct from homogeneous superconductivity [13]. Similarly, neutron scattering experiments [14] reveal superconducting correlations coexisting with stripe fluctuations ('dynamic stripes') that correspond to coupled spin- and charge-density-waves fluctuations. Importantly, pairing correlations without global phase coherence persist up to temperatures of the order of T^* and provide simultaneously diamagnetism, which is observed up to about 150 K in the optimally doped $YBa_2Cu_3O_{7-\delta}$ with $T_c = 92$ K [5]. Hence, the discovered HTS was called unconventional with respect to the weak coupling Bardeen–Cooper–Schrieffer (BCS) theory [15], because it occurs in strongly correlated electron systems, where the Cooper-pair formation is dominated by repulsive electron–electron interactions, that are expected to cause competing and intertwined orders of stripe phases and pair-density waves, electronic liquid-crystal phases, etc. [16]. The phase diagram of the temperature versus the hole doping level for the copper oxides, which contains insulating antiferromagnetic, pseudogap, 'strange metal', superconducting, and Fermi liquid phases in the different doping intervals, is discussed in the reviews, see, e.g., [17]. Thus, turning back to the Q-ball picture, we mention that an essential prerequisite for the Q-balls emergence is the attraction between condensed elementary bosonic spin-/charge-density-wave excitations. It is self-consistently triggered by the formation of Cooper-pairs condensates inside Euclidean Q-balls [1]. Hence, the binding of the fermions into Cooper/local pairs inside the Q-balls occurs via an exchange with semiclassical density fluctuations of a finite amplitude below a high enough temperature T^*. The latter is of the order of the excitation 'mass', i.e., proportional to the inverse of the correlation length of the short-range spin-/charge-density-wave fluctuations. The Q-ball charge Q counts the number of condensed elementary bosonic excitations forming the finite amplitude spin-/charge-density wave inside the Q-ball volume. The amplitude of the Q-ball fluctuation lies in the vicinity of the local minimum of the free energy of the Q-ball, thus making it stable. Euclidean Q-balls arise due to the global invariance of the effective theory under the $U(1)$ phase rotation of the Fourier amplitudes of the spin-/charge-density fluctuations, leading to the conservation of the 'Noether charge' Q in Matsubara time. This is reminiscent of the Q-balls formation in the supersymmetric standard model, where the Noether charge responsible for the baryon number conservation in real time is associated with the $U(1)$ symmetry of the squarks field [18–20]. Contrary to the squark Q-balls, the Euclidean Q-balls arise at finite temperature T^* and the phase of the dominating Fourier component of the spin-/charge-density wave fluctuation rotates with bosonic Matsubara frequency $\Omega = 2\pi T$ in the Euclidean space time. Simultaneously, the local minimum of the Q-ball potential energy located at the finite value of the modulus of the Fourier amplitude arises due to the local/Cooper pairing [2]. A 'bootstrap' condition is an exchange with fluctuations of a finite amplitude that causes the local/Cooper pairing of fermions inside Q-balls already at high temperatures. An idea of a semiclassical 'pairing glue' between fermions in cuprates, but for an itinerant case, was proposed earlier in [21]. Hence, the proposed superconducting pairing mechanism inside Q-balls is distinct from the usual phonon- [22] or spin-fermion coupling models [23] considered previously for high-T_c cuprates, based upon the exchange with infinitesimal spin- and charge-density fluctuations [24] or polarons [25] in the usual Fröhlich picture.

2. Quintessence of Euclidean Q-Balls Picture

In order to derive the explicit relation for the Q-ball charge conservation, one may use [1,2] a simple model Euclidean action S_M with a scalar complex field $M(\tau, \mathbf{r})$, written as:

$$S_M = \int_0^\beta \int_V d\tau d^D\mathbf{r} \frac{1}{g}\Big\{ |\partial_\tau M|^2 + s^2|\partial_\mathbf{r} M|^2 + \mu_0^2|M|^2 + gU_f(|M|^2)\Big\},\ M \equiv M(\tau,\mathbf{r}), \quad (1)$$

where s is bare propagation velocity, and the 'mass' term $\mu_0^2 \sim 1/\xi^2$ is responsible for finite correlation length ξ of the fluctuations. Effective potential energy $U_f(|M|^2)$, as was first derived in [1,2], depends on the field amplitude $|M|$ and contains charge-/spin-fermion coupling constant g in front. $M(\tau + 1/T, \mathbf{r}) = M(\tau, \mathbf{r})$ is periodic function of Matsubara time at finite temperature T [26] and may be considered, e.g., as an amplitude of the SDW/CDW fluctuation with wave vector $\mathbf{Q_{DW}}$:

$$\begin{aligned} &M_{\tau,\mathbf{r}} = M(\tau,\mathbf{r})e^{i\mathbf{Q_{DW}}\cdot\mathbf{r}} + M(\tau,\mathbf{r})^* e^{-i\mathbf{Q_{DW}}\cdot\mathbf{r}}, \\ &M(\tau,\mathbf{r}) \equiv |M(\mathbf{r})|e^{-i\Omega\tau},\ \Omega = 2\pi nT,\ n = 1,2,\ldots \end{aligned} \quad (2)$$

The model (1) is $U(1)$ invariant under the global phase rotation ϕ: $M \to Me^{i\phi}$. Hence, corresponding 'Noether charge' is conserved along the Matsubara time axis. The 'Noether charge' conservation makes possible Matsubara time periodic, finite volume Q-ball semi-classical solutions, that otherwise would be banned in D > 2 by Derrick theorem [27] in the static case. Previously, Q-balls were introduced by Coleman [18] for Minkowski space in QCD and were classified as non-topological solitons [20]. It is straightforward to derive classical dynamics equation for the field $M(\tau, \mathbf{r})$ from Equation (1):

$$\frac{\delta S_M}{\delta M^*(\tau,\mathbf{r})} = -\partial_\tau^2 M(\tau,\mathbf{r}) - s^2 \sum_{\alpha=\mathbf{r}} \partial_\alpha^2 M(\tau,\mathbf{r}) + \mu_0^2 M(\tau,\mathbf{r}) + gM(\tau,\mathbf{r})\frac{\partial U_f}{\partial|M(\tau,\mathbf{r})|^2} = 0. \quad (3)$$

It provides conservation of the 'Noether charge' Q defined via space integral of the Euclidean time component j_τ of the $D+1$-dimensional 'current density' $\{j_\tau, \vec{j}\}$ of the scalar field $M(\tau, \mathbf{r})$:

$$Q = \int_V j_\tau d^D\mathbf{r}\,, \quad (4)$$

where the current density is defined as:

$$j_\alpha = \frac{i}{2}\{M^*(\tau,\mathbf{r})\partial_\alpha M(\tau,\mathbf{r}) - M(\tau,\mathbf{r})\partial_\alpha M^*(\tau,\mathbf{r})\},\ \alpha = \tau,\mathbf{r}. \quad (5)$$

It is straightforward to check that charge Q is conserved for the non-topological field configurations, that occupy finite volume V, i.e., $M(\tau, \mathbf{r} \notin V) \equiv 0$:

$$\frac{\partial Q}{\partial\tau} = \frac{\partial}{\partial\tau}\int_V j_\tau d^D\mathbf{r} = -s^2 \oint_{S(V)} \vec{j}\cdot d\vec{S} = 0\,, \quad (6)$$

Now, approximating the 'Q-ball' field configuration with a step function $\Theta(\mathbf{r})$:

$$M(\tau,\mathbf{r}) = e^{-i\Omega\tau}M\Theta\{\mathbf{r}\}\,;\quad \Theta(\mathbf{r}) \equiv \begin{cases} 1;\ \mathbf{r}\in V; \\ 0;\ \mathbf{r}\notin V. \end{cases} \quad (7)$$

one finds expression for the conserved charge Q:

$$Q = \int_V j_\tau d^D\mathbf{r} = \Omega M^2 V. \quad (8)$$

This relation leads to inverse proportionality between volume V and fluctuation scattering intensity $\sim M^2$ of, e.g., X-ray radiation by the density wave inside a Q-ball, see Equation (18) below.

It is important to mention here that the non-zero charge Q in Equation (8) follows as a result of broken 'charge neutrality' in the choice for the SDW/CDW fluctuation in Equation (2), where periodic dependence on Matsubara time τ enters via an exponential factor with a single sign frequency Ω, rather than in the form of a real function, e.g., $\propto \cos(\Omega\tau + \phi)$. Now, in the step-function approximation of Equation (7), the action S_M equals:

$$S_M = \frac{1}{gT}\left\{\frac{Q^2}{VM^2} + V[\mu_0^2 M^2 + gU_f]\right\}, \tag{9}$$

where Equation (9) is obtained using charge conservation condition Equation (8). It is remarkable that as it follows from the above expression in Equation (9), the Q-ball volume enters in denominator in the $\propto Q^2/V$ term. Hence, provided the $\propto V$ term is positive, there is a minimum of action S_M (free energy) at finite volume V_Q of a Q-ball. Hence, volume V_Q that minimises S_M and energy E_Q equals:

$$V_Q = \frac{Q}{M\sqrt{\mu_0^2 M^2 + gU_f(M)}}\,; \tag{10}$$

$$E_Q = TS_M^{min} = \frac{2Q\sqrt{\mu_0^2 M^2 + gU_f(M)}}{gM} = \frac{2Q\Omega}{g}, \tag{11}$$

where the last equality in Equation (11) follows directly after substitution of expression V_Q from Equation (10) into Equation (8), which then expresses V_Q via Q and Ω. As a result, charge Q cancels in Equation (11), and the following self-consistency equation follows [2]:

$$0 = (\mu_0^2 - \Omega^2)M^2 + gU_f(M). \tag{12}$$

Another self-consistency equation arises from solution of the Eliashberg-like equations with the SDW/CDW fluctuation field $M_{\tau,\mathbf{r}}$ from Equation (2) playing role of the pairing boson [1,2]. Namely, it was also demonstrated in [1,2] that a fermionic spectral gap g_0 inside Euclidean Q-balls arises in the vicinity of the 'nested' regions of the bare Fermi surface (corresponding to the antinodal points of the cuprates Fermi surface) and scales with the local superconducting density n_s inside the Q-balls:

$$g_0 = \sqrt{2M(M-\Omega)}\,;\; n_s = 2|\Psi|^2 \approx \frac{\nu\varepsilon_0}{2}\tanh^2\frac{g_0}{2T}\tanh\frac{2g_0}{3\varepsilon_0}, \tag{13}$$

where $|\Psi|^2$ is local/Cooper-pairs density inside Q-ball [1], and $\nu\varepsilon_0$ is the density of fermionic states involved in 'nesting'. Substitution of Equation (13) into expression for the Q-ball free energy drop due to pairing of fermions leads to the following expression for the pairing-induced effective potential energy $U_{eff}(M)$ of SDW/CDW field [1,2]:

$$U_{eff}(M) \equiv \mu_0^2 M^2 + gU_f = \mu_0^2 M^2 - \frac{4g\nu\varepsilon_0\Omega}{3} I\left(\frac{M}{\Omega}\right),\; M \equiv |M(\tau)| \tag{14}$$

$$I\left(\frac{M}{\Omega}\right) = \int_1^{M/\Omega} d\alpha \frac{\alpha\sqrt{2\alpha(\alpha-1)}}{(1+8\alpha(\alpha-1))}\tanh\frac{\sqrt{2\alpha(\alpha-1)}\Omega}{\varepsilon_0}\tanh\frac{\sqrt{2\alpha(\alpha-1)}\Omega}{2T}. \tag{15}$$

The plot of $U_{eff}(M)$ vs. M/Ω for different temperatures $T \leq T^* = \mu_0/2\pi$ is presented in Figure 1. The figure manifests characteristic Q-ball local minimum at finite amplitude that, in contradistinction with the squarks theory [18], is produced here by condensation of superconducting local/Cooper pairs inside the CDW Q-balls, first arising at temperature

T^*. The minimum deepens down when temperature decreases to $T = T_c$, at which Q-ball volume becomes infinite and bulk superconductivity sets in.

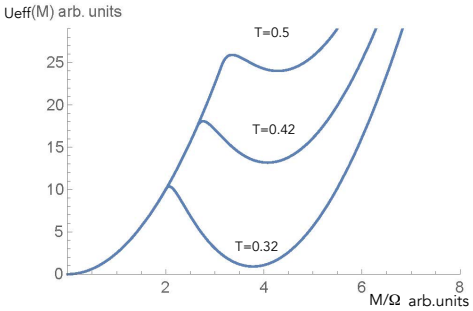

Figure 1. The plots of $U_{eff}(M)$ at different normalised temperatures T/T^* manifesting characteristic Q-ball local energy minimum at finite amplitude due to condensation of local/Cooper pairs inside Q-balls, obtained from Equations (14) and (15), see text.

3. Summary of Theoretical Predictions for Q-Balls

Summarising, Equation (1) was used to describe effective theory of the Fourier components of the leading Q-ball (i.e., short-range) SDW/CDW fluctuations. Explicit expression for $U_f(|M(\tau, \mathbf{r})|)$ was derived and investigated in detail previously [1,2] by integrating out Cooper/local-pairs fluctuations in the 'nested' Hubbard model with charge-/spin-fermion interactions. As a result, Q-ball self-consistency Equation (12) was solved and investigated, and it was established that Euclidean Q-balls describe stable semiclassical short-range charge/spin-ordering fluctuations of finite energy that appear at finite temperatures below some temperature T^*, found to be $T^* \approx \mu_0/2\pi$ [1,2]. Next, it was also found that transition into pseudogap phase at the temperature T^* is of 1st order with respect to the amplitude M of the Q-ball SDW/CDW fluctuation and of 2nd order with respect to the superconducting gap g_0. In particular, the following temperature dependences of these characteristics of the Q-balls were derived from Equations (12), (13) and (15) in the vicinity of the transition temperature T^* into pseudogap phase [2] for the CDW/SDW amplitude:

$$M = \Omega\left(1 + \left(\frac{T^* - T}{\mu_0}\right)^{\frac{2}{5}}\left(\frac{15\mu_0^2}{4\sqrt{2}g\nu}\right)^{\frac{2}{5}}\right), \quad T^* = \frac{\mu_0}{2\pi}, \tag{16}$$

and for the pseudogap g_0:

$$g_0^2 = (T^* - T)^{\frac{2}{5}}\Omega^2\left(\frac{15\mu_0}{g\nu}\right)^{\frac{2}{5}}, \tag{17}$$

which follows after substitution of Equation (16) into Equation (13). These dependences are plotted in Figure 5b in [2].

4. Theoretical Predictions for Some Measurable Q-Balls Manifestations

4.1. Charge Q Conservation

An immediate measurable consequence of the Q-ball charge conservation in a form of Equation (8) would be inverse correlation at fixed temperature $T = \Omega/2\pi$ between Q-ball volume $V_Q = 4\pi R_Q^3/3$ and amplitude squared M^2, which can then be, respectively, associated with the coherence length $\xi^3 \sim {R_Q}^3 \sim V_Q$ and amplitude $A \sim M^2$ of the X-ray scattering peak [26] from the Q-balls in the pseudogap phase of high-T_c cuprates, see Figure 2:

$$\xi^3 \sim V_Q = \left(\frac{Q}{\Omega}\right)\frac{1}{M^2} \sim \left(\frac{Q}{\Omega}\right)\frac{1}{A}. \tag{18}$$

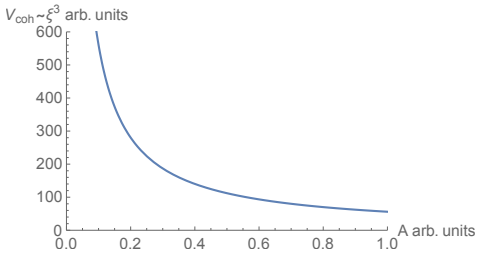

Figure 2. Q-ball volume $V_Q \sim \xi^3$ as function of the CDW/SDW amplitude squared $M^2 \sim A$ (normalised) is plotted in the arbitrary units using Equation (18). Here, coherence volume ξ^3 and amplitude A are characteristics of the X-ray scattering peak from the Q-balls in the pseudogap phase of high-T_c cuprates, see text.

This plot is in good qualitative correspondence with Figure 3a of the experimental data of the X-ray scattering in high-T_c cuprates $HgBa_2CuO_{4+y}$ [3].

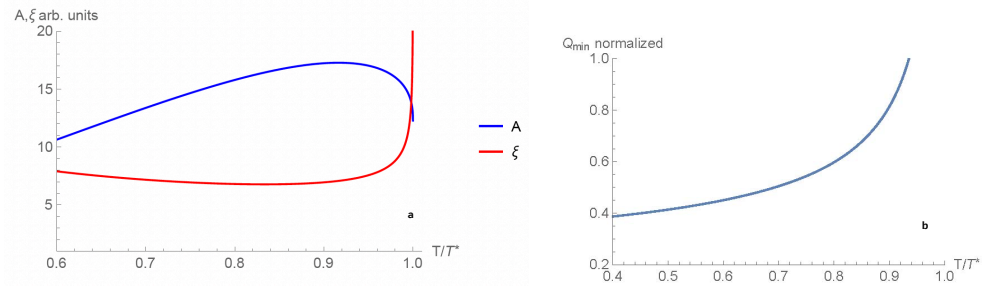

Figure 3. (**a**) Theoretical temperature dependences of the SDW/CDW amplitude $M^2 = A$ (blue curve) and Q-ball size $R = \xi$ (red curve), temperature expressed in units of $T^* = \mu_0/2\pi$; (**b**) temperature dependence of the smallest Q-ball charge Q_{min} from Equation (26), see text. Corresponding experimental data points are presented in G. Campi et al. paper [3].

4.2. Manifestations of Superconducting Condensates Inside Q-Balls

Strikingly, but it follows from Equation (17), that micro X-ray diffraction data also allow to infer an emergence of superconducting condensates inside the Q-balls below T^*. The reason is in the inflation of the volume, which is necessary to stabilise the superconducting condensate at vanishing density. Indeed, this is the most straightforward to infer from linearised Ginzburg–Landau (GL) equation [28] for the superconducting order parameter Ψ of a Q-ball of radius R in the spherical coordinates:

$$-\frac{\hbar^2}{4m}\ddot{\chi} = bg_0^2\chi\,; \quad \Psi(\rho) = \frac{C\chi(\rho)}{\rho}\,; \quad \Psi(R) = 0, \tag{19}$$

where g_0^2 from Equation (13) substitutes GL parameter $a = \alpha \cdot (T_c - T)/T_c$ modulo dimensionful constant b of GL free energy functional [28]. Then, it follows directly from solution of Equation (19):

$$\chi \propto \sin(k_n\rho)\,; \quad Rk_n = \pi n,\,; \quad n = 1, 2, \ldots, \tag{20}$$

that Equation (19) would possess solution (20) with the eigenvalue bg_0^2 only if the Q-ball radius is greater than R_{min}:

$$\frac{\hbar^2}{4m}\left(\frac{\pi}{R_{min}}\right)^2 = bg_0^2. \tag{21}$$

Hence, due to conservation condition Equation (8), charge Q should obey the following condition:

$$Q \geq Q_{min} \equiv \Omega M^2 (R_m)^3 = \Omega M^2 \frac{(\pi\hbar)^3}{g_0^3(4mb)^{3/2}}\,. \tag{22}$$

This would have an immediate influence on the temperature dependence of the most probable value of charge Q. The letter value could be evaluated using expression for the Q-ball energy Equation (11): $E_Q = 2Q\Omega/g$ obtained in [1]. Then, Boltzmann distribution of energies of the Q-balls 'gas' indicates that the most numerous, i.e., the most probable to occur, Q-balls are those with the smallest possible charge Q, and their respective population (overage) number $\bar{n}_Q$ in unit volume of the sample is:

$$\bar{n}_Q \propto \frac{1}{V} G_Q \exp\left\{-\frac{E_Q}{k_B T}\right\} = G_Q \exp\left\{-\frac{2Q\Omega}{g k_B T}\right\}, G_Q = \frac{V}{V_Q}, \tag{23}$$

where G_Q counts the number of possible Q-ball 'positions' in the sample of volume V, V_Q being Q-ball volume, and $\Omega/k_B T = 2\pi$. Hence, Equation (23) indicates that the Boltzmann's exponent is greater for smaller Q. On the other hand, due to accommodated superconducting condensates inside the Q-balls, their Noether charge Q is limited from below by Q_{min}, as demands Equation (22). Substituting into Equations (21) and (22) temperature dependences of M and g_0 from Equations (16) and (17), one finds:

$$R_{min} = \frac{1}{\Omega(T^* - T)^{1/5}} \frac{\pi\hbar}{\sqrt{4mb}} \left(\frac{g\nu}{15\mu_0}\right)^{1/5}; \tag{24}$$

$$A \propto M^2 = \Omega^2 \left(1 + \left(\frac{T^* - T}{\mu_0}\right)^{\frac{2}{5}} \left(\frac{15\mu_0^2}{4\sqrt{2}g\nu}\right)^{\frac{2}{5}}\right)^2; \tag{25}$$

$$Q_{min} = \left(1 + \left(\frac{T^* - T}{\mu_0}\right)^{\frac{2}{5}} \left(\frac{15\mu_0^2}{4\sqrt{2}g\nu}\right)^{\frac{2}{5}}\right)^2 \frac{(\pi\hbar)^3}{(4mb)^{3/2}(T^* - T)^{3/5}} \left(\frac{g\nu}{15\mu_0}\right)^{3/5} \tag{26}$$

Taking into account the above-mentioned proportionality between M^2 and the amplitude A of the X-ray scattering peak, and using Equations (24)–(26), one obtains plots of the temperature dependences of a single Q-ball scattering amplitude $A \approx M^2$ and coherence length $\xi \approx R_{min}$, Figure 3a, as well as of the temperature dependence of the smallest Q-ball charge Q_{min} in Figure 3b. Finally, in Figure 4, theoretical prediction for the temperature dependence of weighted scattering amplitude A_w is presented. Namely, the single Q-ball scattering amplitude A from Equation (25) is multiplied by the Q-balls population number $\bar{n}_Q$ from Equation (23): $A_w = A\bar{n}_Q$, where $Q = Q_{min}$ is given by Equation (26).

Experimental data points from paper [3] are in good accord with the theoretical curves in Figures 3b and 4.

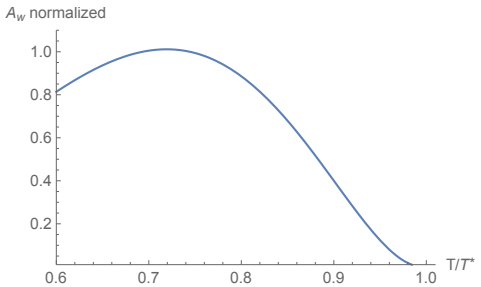

Figure 4. Theoretical prediction for the temperature dependence of the weighted scattering amplitude A_w, see text, in the units of $T^* = \mu_0/2\pi$.

5. Conclusions

To summarise, some measurable manifestations of the previously proposed theory [1,2] of the Q-ball mechanism of high-T_c superconductivity are derived. In particular, it is demonstrated that Euclidean Q-ball charge conservation leads to an inverse correlation between the Q-ball volume and X-ray scattering amplitude. In addition, the proposed

theory predicts that superconducting condensate, which forms self-consistently inside a Q-ball together with a semiclassical CDW/SDW short-range fluctuation, manifests itself in a peculiar sharp inflation of the Q-ball radius at T^*, where the density of the superconducting condensate inside the Q-balls tends to zero. This follows directly from the Ginzburg–Landau theory for the radius of a superconducting sphere in the vicinity of the transition temperature T_c, which for an individual Q-ball coincides with T^*. As the measurable consequence, the width of the X-ray coherence peak in momentum space, being inverse proportional to the Q-ball radius, decreases when the temperature approaches T^* from below. Simultaneously, the X-ray scattering amplitude, being proportional to the square of the CDW/SDW fluctuation amplitude inside the Q-ball, first sharply increases below T^* and then develops a maximum as the temperature farther decreases. These predictions follow from the previously found [1,2] mixed nature of the transition into the pseudogap phase at T^*. Namely, while an amplitude of the CDW/SDW fluctuation inside emerging Q-balls is finite at the transition, the density of the simultaneously emerging superconducting condensate inside the Q-balls is infinitesimally small at T^* and rapidly grows below this transition temperature. This causes the fast deflation of the Q-ball radius at temperatures immediately below T^*. The theoretical predictions favourably compare with the experimental data from the micro X-ray diffraction [3,4]. Finally, it is worth mentioning several other theoretical works that considered the condensation of (bi)polarons in HTS cuprates [29–31] and supersolid-to-superfluid transitions in the phase-separated supersolid stripe/strings and superconducting stripes. None of these theories have considered the conservation of the 'Noether charge' Q along the Matsubara time axis that, together with the energy conservation, provides Q-ball solutions of a finite volume below high-T^* temperatures. In addition, the here-presented Q-ball model of high-T_c superconductivity in cuprates is distinct from the model presented recently [32], where the lattice field models known from high-energy physics, including magnetic monopoles, dyons, and their confinement, are projected onto the model of a granular superconductor. While Q-balls are non-topological solitonic quasi-classical solutions minimising the Euclidean action of the scalar field [20] in the state with no long-range order, the magnetic monopoles and dyons considered in [32] are instantons that connect degenerate long-range-ordered vacua. Moreover, the pseudogap predicted in the present Q-ball theory is in the fermionic spectrum, and it is induced by the condensation of strongly coupled fermionic pairs that possess a wave function being non-zero only in the vicinity of the 'antinodal' points in the Brillouin zone. The shape of the Cooper pair is 'starfish' like [1]: it is characterised by the length scale v_f/g_0 in the antinodal direction and by the Q-ball radius in the 'nodal' direction, in qualitative correspondence with the experiment [33]. Another important distinction between the previous theories of high-T_c cuprates and the present Q-ball theory is that the latter introduces a 'bootstrap' condition: the emergence of pairing 'glue', built from condensed-with-finite-amplitude-attracting bosonic fluctuations inside a Q-ball, and Cooper/local pairs condensation inside the Q-ball are self-consistent events. Further, an exchange with fluctuations of a finite amplitude constituting a Q-ball causes the local/Cooper pairing of fermions inside the Q-ball volume at higher temperatures then the usual Fröhlich mechanism of exchange with infinitesimal 'glue' bosons of any types exploited since the BCS theory was proposed, as was mentioned in the Introduction. An idea of a semiclassical 'pairing glue' between fermions in cuprates, but for an itinerant case, was proposed earlier in [21].

Funding: This research was in part supported by Grant No. K2-2022-025 in the framework of the Increase Competitiveness Program of NUST MISIS.

Data Availability Statement: Not applicable.

Acknowledgments: The author is grateful to Antonio Bianconi for making available the experimental data on micro X-ray diffraction in high-T_c cuprates prior to publication and very fruitful detailed discussions.

Conflicts of Interest: The author declares no conflict of interest.

References

1. Mukhin, S.I. Euclidean Q-Balls of Fluctuating SDW/CDW in the 'Nested' Hubbard Model of High-Tc Superconductors as the Origin of Pseudogap and Superconducting Behaviors. *Condens. Matter* **2022**, *7*, 31. [CrossRef]
2. Mukhin, S.I. Euclidean Q-balls of electronic spin/charge densities confining superconducting condensates as the origin of pseudogap and high-Tc superconducting behaviours. *Ann. Phys.* **2022**, *447*, 169000. [CrossRef]
3. Campi, G.; Barba, L.; Zhigadlo, N.D.; Ivanov, A.A.; Menushenkov, A.P.; Bianconi, A. Q-Balls in the pseudogap phase of Superconducting $HgBa_2CuO_{4+y}$. *Condens. Matter* **2022**, *8*, 15.
4. Campi, G.; Bianconi, A.; Poccia, N.; Bianconi, G.; Barba, L.; Arrighetti, G.; Innocenti, D.; Karpinski, J.; Zhigadlo, N.D.; Kazakov, S.M.; et al. Inhomogeneity of charge-density-wave order and quenched disorder in a high-Tc superconductor. *Nature* **2015**, *525*, 359–362. [CrossRef]
5. Li, L.; Wang, Y.; Komiya, S.; Ono, S.; Ando, Y.; Gu, G.D.; Ong, N.P. Diamagnetism and Cooper pairing above Tc in cuprates. *Phys. Rev. B* **2010**, *81*, 054510. [CrossRef]
6. Uemura, Y.J.; Luke, G.M.; Sternlieb, B.J.; Brewer, J.H.; Carolan, J.F.; Hardy, W.; Yu, X.H. Universal correlations between Tc and n_s/m^* in high-Tc cuprate superconductors. *Phys. Rev. Lett.* **1989**, *62*, 2317–2320. [CrossRef]
7. Bednorz, J.G.; Müller, K.A. Possible highTc superconductivity in the Ba-La-Cu-O system. *Z. Phys. B* **1986**, *64*, 189. [CrossRef]
8. Gao, L.; Xue, Y.Y.; Chen, F.; Xiong, Q.; Meng, R.L.; Ramirez, D.; Chu, C.W.; Eggert, J.H.; Mao, H.K. Superconductivity up to 164 K in $HgBa_2Ca_{m-1}Cu_mO_{2m+2+\delta}$ (m = 1, 2, and 3) under quasihydrostatic pressures. *Phys. Rev. B* **1994**, *50*, 4260. [CrossRef]
9. Nagamatsu, J.; Nakagawa, N.; Muranaka, T.; Zenitani, Y.; Akimitsu, J. Superconductivity at 39 K in magnesium diboride. *Nature* **2001**, *410*, 63. [CrossRef]
10. Kamihara, Y.; Hiramatsu, H.; Hirano, M.; Kawamura, R.; Yanagi, H.; Kamiya, T.; Hosono, H. Iron-Based Layered Superconductor: LaOFeP. *J. Am. Chem. Soc.* **2006**, *128*, 10012. [CrossRef]
11. Ozawa, T.C.; Kauzlarich, S.M.; Chemistry of layered d-metal pnictide oxides and their potential as candidates for new superconductors. *Sci. Technol. Adv. Mater.* **2008**, *9*, 033003. [CrossRef] [PubMed]
12. Hashimoto, M.; He, R.-H.; Tanaka, K.; Testaud, J.-P.; Meevasana, W.; Moore, R.G.; Lu, D.; Yao, H.; Yoshida, Y.; Eisaki, H.; et al. Particle—Hole symmetry breaking in the pseudogap state of Bi2201. *Nat. Phys.* **2010**, *6*, 414. [CrossRef]
13. Davis, J.C.S.; Lee, D.-H. Concepts relating magnetic interactions, intertwined electronic orders, and strongly correlated superconductivity. *Proc. Natl. Acad. Sci. USA* **2013**, *110*, 17623. [CrossRef]
14. Tranquada, J.M.; Gu, G.D.; Hücker, M.; Jie, Q.; Kang, H.-J.; Klingeler, R.; Li, Q.; Tristan, N.; Wen, J.S.; Xu, G.Y.; et al. Evidence for unusual superconducting correlations coexisting with stripe order in $La_{1.875}Ba_{0.125}CuO_4$. *Phys. Rev. B* **2008**, *78*, 174529. [CrossRef]
15. Bardeen, J.; Cooper, L.N.; Schrieffer, J.R. Microscopic Theory of Superconductivity. *Phys. Rev.* **1957**, *106*, 162. [CrossRef]
16. Fradkin, E.; Kivelson, S.A.; Tranquada, J.M. Colloquium: Theory of intertwined orders in high temperature superconductors. *Rev. Mod. Phys.* **2015**, *87*, 457. [CrossRef]
17. Keimer, B.; Kivelson, S.; Norman, M.; Uchida, S.; Zaanen, J. From quantum matter to high-temperature superconductivity in copper oxides. *Nature* **2015**, *518*, 179. [CrossRef]
18. Coleman, S.R. Q-balls. *Nuclear Phys. B* **1985**, *262*, 263–283. [CrossRef]
19. Rosen, G. Particlelike Solutions to Nonlinear Complex Scalar Field Theories with PositiveDefinite Energy Densities. *J. Math. Phys.* **1968**, *9*, 996. [CrossRef]
20. Lee, T.D.; Pang, Y. Nontopological solitons. *Phys. Rep.* **1992**, *221*, 251–350. [CrossRef]
21. Mukhin, S.I. Negative Energy Antiferromagnetic Instantons Forming Cooper-Pairing Glue and Hidden Order in High-Tc Cuprates. *Condens. Matter* **2018**, *3*, 39. [CrossRef]
22. Eliashberg, G.M. Interactions between electrons and lattice vibrations in a superconductor. *JETP* **1960**, *11*, 696–702.
23. Abanov, A.; Chubukov, A.V.; Schmalian, J. Quantum-critical theory of the spin-fermion model and its application to cuprates: Normal state analysis. *Adv. Phys.* **2003**, *52*, 119–218. [CrossRef]
24. Seibold, G.; Arpaia, R.; Peng, Y.Y.; Fumagalli, R.; Braicovich, L.; Di Castro, C.; Caprara, S. Strange metal behaviour from charge density fluctuations in cuprates. *Commun. Phys.* **2021**, *4*, 7. [CrossRef]
25. Bianconi, A.; Missori, M. The instability of a 2D electron gas near the critical density for a Wigner polaron crystal giving the quantum state of cuprate superconductors. *Solid State Commun.* **1994**, *91*, 287–293. [CrossRef]
26. Abrikosov, A.A.; Gor'kov, L.P.; Dzyaloshinski, I.E. *Methods of Quantum Field Theory in Statistical Physics*; Dover Publications: New York, NY, USA, 1963.
27. Derrick, G.H. Comments on nonlinear wave equations as models for elementary particles. *J. Math. Phys.* **1964**, *5*, 1252–1254. [CrossRef]
28. Abrikosov, A.A. *Fundamentals of the Theory of Metals*; Elsevier Science Publishers B.V.: Amsterdam, The Netherlands, 1988; Chapter 17.
29. Kusmartsev, F.V.; Castro, D.D.; Bianconi, G.; Bianconi, A. Transformation of strings into an inhomogeneous phase of stripes and itinerant carriers. *Phys. Lett. A* **2000**, *275*, 118–123. [CrossRef]
30. Masella, G.; Angelone, A.; Mezzacapo, F.; Pupillo, G.; Prokof'ev, N.V. Supersolid Stripe Crystal from Finite-Range Interactions on a Lattice. *Phys. Rev. Lett.* **2019**, *123*, 045301. [CrossRef]
31. Innocenti, D.; Ricci, A.; Poccia, N.; Campi, G.; Fratini, M.; Bianconi, A. A Model for Liquid-Striped Liquid Phase Separation in Liquids of Anisotropic Polarons. *J. Supercond. Nov. Magn.* **2009**, *22*, 529–533. [CrossRef]

32. Trugenberger, C.A. Magnetic Monopoles, Dyons and Confinement in Quantum Matter. *Condens. Matter* **2023**, *8*, 2. [CrossRef]
33. Li, H.; Zhou, X.; Parham, S.; Gordon, K.N.; Zhong, R.D.; Schneeloch, J.; Gu, G.D.; Huang, Y.; Berger, H.; Arnold, G.B.; et al. Four-legged starfish-shaped Cooper pairs with ultrashort antinodal length scales in cuprate superconductors. *arXiv* **2018**, arXiv:1809.02194.

Disclaimer/Publisher's Note: The statements, opinions and data contained in all publications are solely those of the individual author(s) and contributor(s) and not of MDPI and/or the editor(s). MDPI and/or the editor(s) disclaim responsibility for any injury to people or property resulting from any ideas, methods, instructions or products referred to in the content.